ENERGY SPREAD ISSUE IN LASER UNDULATOR BASED XFELs*

Yujong Kim†, Y. C. Jing, S. Y. Lee, and P. E. Sokol
Indiana University, Bloomington, IN 47408, USA

Abstract

At the Center for the Exploration of Energy and Matter (CEEM) in Indiana University, we have been developing a new XFEL concept, which is based on inverse Compton scattering and a laser undulator instead of the conventional magnetic undulator. In this paper, we report an estimation of the energy spread growth in the electron storage ring due to the inverse Compton scattering itself and their impacts on the FEL lasing in the laser undulator based XFEL concept.

INTRODUCTION

After the successful operation of short-wavelength Free Electron Laser (FEL) facilities at SPring-8 (SCSS) in Japan, DESY (FLASH) in Germany, and SLAC (LCLS) in the USA, many laboratories around the world are eager to build their own X-ray FEL (XFEL) facilities, which can supply coherent, ultra-bright, and femtosecond or attosecond long hard X-rays. With advanced next generation X-rays, we can open femto-sciences in biology and chemistry and various new research fields in physics, structural biology, and material science where the femtosecond temporal and atomic-scale spatial resolutions are required. To construct such an XFEL facility, however, a long linac with an energy of several GeV and a long undulator with a length of several tens of meters are required. Recently, several research groups have been studying Inverse Compton Scattering (ICS) and laser undulator based new compact XFEL concept [1–4]. Since the period of the laser undulator is about 500 nm, an ultra-compact XFEL facility may be possible with a relatively low energy 25 MeV electron accelerator.

To study the survivability of modern microelectronic technologies in space or in man-made high threat environments, the Crane Division of Naval Surface Warfare Center (NSWC) and CEEM have been constructing the Advanced eLectron-PHoton fAcility (ALPHA) at Indiana University. The ALPHA facility will consist of a 50 MeV electron linac and a compact electron storage ring with a circumference of 20 m [5]. The primary focus for ALPHA is electron based radiation effects testing. However, there is also an interest in high intensity X-rays, and we are exploring the feasibility of using a laser undulator based compact XFEL for this testing. In this paper, we describe possible parameters of the ALPHA storage ring for the ICS and laser undulator based XFEL facility. Then, we report the impact of the energy spread growth due to the ICS itself on the FEL lasing.

LASER UNDULATOR BASED XFEL

A conventional undulator is a periodic structure of permanent dipole magnets supplying an alternating static magnetic field along the undulator. Generally, the period of the conventional undulator λ_u is about a few tens of millimeters. When electron beams go through the undulator, they perform a wiggling motion, which induces changes in the transverse momentum of the electron beam and generates spontaneous undulator radiation at a resonance wavelength λ_x. For the on-axis radiation propagation of a conventional planar undulator, the resonant wavelength λ_x is given by

$$\lambda_x = \frac{\lambda_u}{2\gamma^2}(1 + \frac{K^2}{2}), \qquad (1)$$

$$K = \frac{eB\lambda_u}{2\pi m_e c} = 0.934B[\mathrm{T}]\lambda_u[\mathrm{cm}], \qquad (2)$$

where γ is the beam energy in units of the electron rest energy $m_e c^2$, e is the electron charge, and B is the peak magnetic field. In addition, there are interactions between the spontaneous undulator radiation and the electron beams which go through the undulator. Depending on the relative phase between the electrons and the plane wave of the undulator radiation, electrons can gain or loose energy due to the undulator radiation. Under this condition, the so-called longitudinal density modulation, or FEL microbunching instability can occur if highly dense and cold electron beams with a low slice emittance, a low slice energy spread, and a high peak current are sent to the undulator. Emitted photon beams from these microbunching structures are in-phase or coherent, and the emitted radiation power is exponentially amplified along the undulator, which is the working principle of coherent ultra-brightness, ultra-fast SASE mode XFEL with a conventional undulator. In case of the LCLS project, a conventional undulator with $\lambda_u = 30$ mm and $K \simeq 3.5$ and a long 13.6 GeV electron linac are used to generate coherent XFEL photon beams at 0.15 nm [6].

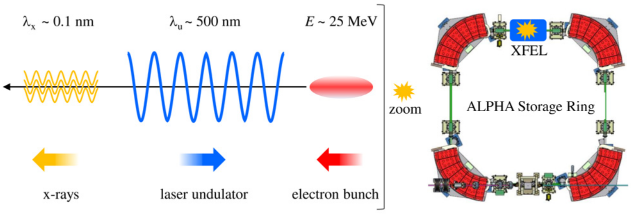

Figure 1: Layout of an XFEL at the ALPHA facility.

---

* This work has been partially supported under Grant N00164-08-GM03 P00004 from the Naval Surface Warfare Center Crane Division.

† ykim68@indiana.edu

Table 1: Parameters of an XFEL at the ALPHA facility.

Parameters	Unit	Value
electron beam energy	MeV	25
bending radius of storage ring dipole	m	1.273
circumference of the storage ring	m	20
electron revolution frequency	MHz	15
single bunch charge	nC	10
peak current	A	400
rms bunch length	ps	10
rms electron beamsize in laser undulator	μm	100
β-function at laser undulator	m	0.1
normalized rms emittance	μm	5
rms slice energy spread without ICS	10^{-5}	1.9
wavelength of laser undulator	μm	1
period of laser undulator	nm	500
length of laser undulator	ps	10
electron and laser interaction frequency	MHz	15
wavelength of X-ray photon	nm	0.1
minimum rms spotsize of laser undulator	μm	100

According to Eq. (1), the hard X-ray photon beams can also be generated at $\lambda_x \simeq 0.1$ nm with a much lower electron beam energy if the undulator period is ultra-short. Since a laser beam has an alternating periodic magnetic field, the laser beam can also be considered as an undulator to generate the hard X-rays. By sending electron beams into the laser beam, which is known as the inverse Compton scattering, we can also generate hard X-rays with the laser undulator. In this case, the period of the laser undulator λ_u is half of the laser wavelength λ_L because the alternating magnetic field in the laser undulator and electron beams are moving simultaneously and approaching to each other with the speed of light. Additionally, the undulator deflection parameter K of the linearly polarized laser beams is given by

$$K = \frac{eB_u\lambda_L}{4\pi m_e c} \simeq 8.55\times 10^{-10}\lambda_L[\mu\mathrm{m}]\sqrt{I[\mathrm{W/cm}^2]}\,, \quad (3)$$

$$I = P/\pi r^2\,, \quad (4)$$

where B_u is the peak magnetic field of the laser undulator, I is the laser intensity, P is the laser power, and r is the radius of the uniform flat-top laser beam profile [1–3]. Therefore, the incoherent spontaneous undulator radiation can be generated at $\lambda_x \simeq 0.1$ nm with 25 MeV electron beams and an ultra-short laser undulator with $\lambda_u = 500$ nm, $\lambda_L = 2\lambda_u = 1$ μm as shown in Fig. 1 [7]. If the electron beam quality is high enough to allow the FEL microbunching instability, the power can be enhanced in the laser undulator, and coherent FEL photon beams can be generated at $\lambda_x \simeq 0.1$ nm [1–3].

Generally, it is not easy to obtain saturation of the FEL photon beam power in a single path due to the short laser undulator length of about 10 ps (FW). To overcome this short undulator length, a storage ring can be used to get the FEL power saturation in multi-turns. But the saturation is reachable only if the quality of electron beams is continuously conserved to develop the microbunching instability in multi-turns while electron beams circulate in the storage ring. This is the laser undulator based XFEL concept which uses a compact electron storage ring and a high power laser for the inverse Compton scattering. A possible layout of the laser undulator based XFEL at the ALPHA facility is shown in Fig. 1, and its parameters are summarized in Table 1. Since it is a storage ring based facility with a high repetition rate of 15 MHz, the average power of X-rays can be higher than the normal linac based facilities.

ENERGY SPREAD ISSUE IN XFEL

To develop the FEL microbunching instability and eventually to reach power saturation, the beam quality should be continuously conserved as the electron beams circulate the storage ring. Specially, to keep the gain length and saturation length reasonably short, the slice energy spread should be smaller than the FEL parameter ρ_{FEL} which is given by

$$\rho_{\mathrm{FEL}} = \frac{1}{4}\left[\frac{1}{\pi^2}\frac{I_{pk}}{I_A}\frac{K^2[JJ]^2}{\gamma}\frac{\lambda_u^2}{\varepsilon_{nx}^2\beta_x^2}\right]^{1/3}, \quad (5)$$

where I_{pk} is the peak current, $I_A = 17045$ A is the Alfven current, $[JJ]^2 = [J_0(\xi) - J_1(\xi)]^2$ where J_0 and J_1 are the Bessel function, and $\xi = K^2/(4+2K^2)$, ε_{nx} is the normalized horizontal emittance, β_x is the horizontal β-function [6]. Generally, the equilibrium energy spread in a storage ring is determined when the radiation damping rate due to the synchrotron radiation is same as the quantum excitation rate [8]. By using the synchrotron radiation integrals $(I_1 - I_5)$, we can estimate the equilibrium rms relative energy spread due to the synchrotron radiation from the storage ring dipole magnets [8–11]. For a planar isomagnetic ring, the equilibrium energy spread is given by

$$\sigma_\delta^2 = C_q\frac{\gamma^2}{J_s\rho_o}\,, \quad (6)$$

where $C_q = 55\hbar/(32\sqrt{3}m_e c) = 3.83\times 10^{-13}$ m, $J_s \approx 2$ is the longitudinal damping partition number, and ρ_o is the bending radius of the storage ring dipole magnets [8–11]. In case of the ALPHA storage ring, the initial slice energy spread is same as the equilibrium rms relative energy spread σ_δ because the energy chirp in the longitudinal phase space is negligible. As summarized in Table 1, the slice energy spread is about 1.9×10^{-5} without operation of any insertion device (ID). However, the slice energy spread is changed if there is an additional operating ID in the storage ring due to the changed radiation damping and quantum excitation rates. Since the laser undulator can be considered as an insertion device (ID) in the ALPHA storage ring, we can also estimate the growth of the rms relative energy spread due to the laser undulator by using the synchrotron radiation integrals [9–11]. The changed energy spread $\sigma_{\delta,u}$ due to the linearly polarized laser undulator is given by

$$\left(\frac{\sigma_{\delta,u}}{\sigma_\delta}\right)^2 = \frac{1+\frac{I_{3,u}}{I_3}}{1+\frac{2I_{2,u}+I_{4,u}}{2I_2+I_4}} \approx \frac{1+\frac{4}{3\pi}\frac{L_u}{2\pi\rho_o}\frac{\rho_o^3}{\rho_u^3}}{1+\frac{1}{2}\frac{L_u}{2\pi\rho_o}\frac{\rho_o^2}{\rho_u^2}}\,, \tag{7}$$

$$I_2 = \oint_{ring} \frac{1}{\rho^2} ds = \frac{2\pi}{\rho_o}\,, \tag{8}$$

$$I_3 = \oint_{ring} |\frac{1}{\rho}|^3 ds = \frac{2\pi}{\rho_o^2}\,, \tag{9}$$

$$I_4 = \oint_{ring} \frac{(1-2n)\eta_x}{\rho^3} ds \approx 0\,, \tag{10}$$

$$I_{2,u} = \int \frac{\cos^2(k_u s)}{\rho_u^2} ds = \frac{L_u}{2\rho_u^2}\,, \tag{11}$$

$$I_{3,u} = \int \frac{|\cos^3(k_u s)|}{\rho_u^3} ds = \frac{4L_u}{3\pi\rho_u^3}\,, \tag{12}$$

$$\begin{aligned} I_{4,u} &= -\int \frac{\cos^4(k_u s)}{\rho_u^4 k_u^2} ds \\ &\quad +2\int \frac{\sin^2(k_u s)\cos^2(k_u s)}{\rho_u^4 k_u^2} ds\,, \\ &= -\frac{L_u}{8\rho_u^4 k_u^2} \ll I_2,\, I_{2,u}\,, \end{aligned} \tag{13}$$

where $n(s) = -\rho(s)(\partial B/\partial\rho)/B$ is the field index, $\eta_x(s)$ is the horizontal dispersion, $\rho(s)$ is the radius of curvature of the design orbit, $\rho(s) = \rho_o = 1.273$ m in the storage ring dipoles, s is the coordinate along the storage ring, $k_u = 2\pi/\lambda_u$ is the wave number of the laser undulator, ρ_u is the bending radius in the laser undulator, $L_u = 3$ mm is the length of the laser undulator.

From Eqs. (3), (6), and (7) and $\rho_u[\mathrm{m}] \simeq p[\mathrm{GeV/c}]/(0.2998 B_u[\mathrm{T}])$ where p is the momentum of electron beams, we can estimate the slice energy spread change in the storage ring due to operation of the laser undulator or ICS itself. Since the FEL parameter ρ_{FEL} is a function of the undulator deflection parameter K as shown in Eq. (5), the FEL parameter is also changed according to the laser intensity or power of the laser undulator [6]. Similarly, ρ_u is also a function of B_u and hence the laser intensity or power as shown in Eqs. (3) and (4). Therefore, we can find a trend of the FEL parameter and the slice energy spread with respect to the laser intensity or power. As shown in Fig. 2, the slice energy spread is always much larger than the FEL parameters for all power ranges of the laser undulator. Therefore the FEL microbunching instability can not be developed continuously in multi-turns if the laser undulator is used to generate the XFEL photon beams. Note that we did not consider the emittance growth in ρ_{FEL} due to the laser undulator or ICS itself. If we consider the slice energy spread growth and the slice emittance growth due to the intra-beam scattering and the ICS itself, the gap between the slice energy spread and the FEL parameter will be much larger than that in Fig. 2. This means that the saturation length will be dramatically increased if we use the laser undulator for the XFEL lasing [6].

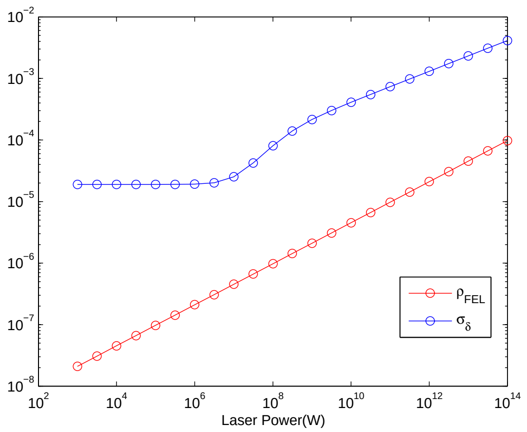

Figure 2: The FEL parameter and the relative rms slice energy spread with respect to the laser power.

SUMMARY

We have studied the feasibility of a laser undulator and the ALPHA storage ring based compact XFEL facility. It will be difficult to generate coherent XFEL photon beams due to the large slice energy spread growth, which is generated by the inverse Compton scattering itself. Generally, we can get a much higher peak current, a much smaller slice emittance, and a much smaller slice energy spread with a linear accelerator. Therefore, in the near future, we will also check the possibility of the laser undulator based XFEL concept which uses a low energy electron linear accelerator instead of a storage ring.

REFERENCES

[1] P. Sprangle *et al.*, J. Appl. Phys. **72**, p. 5032 (1992).

[2] P. Sprangle *et al.*, Phys. Fluids B. **4**, p. 2241 (1992).

[3] P. Sprangle *et al.*, Phys. Rev. ST Accel. Beams **12**, 050702 (2009).

[4] R. Bonifacio *et al.*, Nucl. Instr. and Meth. A **593** p. 69 (2008).

[5] S. Y. Lee *et al.*, Rev. Sci. Instrum. **74**, 075107 (2007).

[6] LCLS design study group, SLAC Report No. SLAC-R-593, 2002.

[7] M. Bech *et al.*, J. Synchrotron Rad. **16**, p. 43 (2009).

[8] M. Sands, SLAC Report No. SLAC-R-121, 1979.

[9] R. H. Helm *et al.*, IEEE Trans. Nucl. Sci. **NS-20**, p. 900 (1973).

[10] R. P. Walker, CERN Report No. CERN-95-06 v2, p. 807, 1995.

[11] M. H. Wang *et al.*, Rev. Sci. Instrum. **78**, 055109 (2007).